

## Swelling behavior and local topology of an $L_3$ (sponge) phase

A. Maldonado,<sup>1</sup> W. Urbach,<sup>1</sup> R. Ober,<sup>2</sup> and D. Langevin<sup>1</sup>

<sup>1</sup>Laboratoire de Physique Statistique (CNRS URA 1306), Ecole Normale Supérieure, 24, rue Lhomond, 75231 Paris Cedex 05, France

<sup>2</sup>Laboratoire de Physique de la Matière Condensée, Collège de France, 11, place Marcelin-Berthelot,

75231 Paris Cedex 05, France

(Received 12 June 1995)

The swelling behavior of an  $L_3$  (sponge) surfactant phase was studied by the small angle x-ray scattering technique; we show that it is well described by the recently computed swelling law for minimal surfaces. In addition, the self-diffusion coefficient  $D_S$  of several probes within the bilayers of the  $L_3$  phase was measured by the fluorescent recovery after fringe pattern photobleaching technique. The variation of  $D_S$  with the surfactant volume fraction provides a clue for the topology of the surface over which the midsurface of the bilayers is draped. This allows us to determine the location of the neutral surface near the polar-apolar interface of the bilayers. [S1063-651X(96)12207-8]

PACS number(s): 61.10.Eq, 61.30.Eb, 66.10.Cb, 82.70.Kj

### I. INTRODUCTION

The study of the physical properties of lyotropic surfactant phases has attracted a lot of interest in the last years. The structure of several phases is now well understood. For example, for many binary surfactant-water systems in the dilute regime, it is known that the amphiphilic molecules aggregate and form micelles whose size and shape are well characterized by light, x-ray, and neutron scattering [11].

In the more concentrated regime, some of these systems display connected structures in which a continuous surfactant bilayer divides regions of space filled with solvent. In the cubic phases, like in a solid crystal, one can have different space symmetries as well as different topologies; some of them have been reported in the literature [2]. The small angle x-ray scattering technique (SAXS) can be used to measure the lattice space characteristic of the unit cell of the phase [3].

The spongelike or  $L_3$  phase [4] can be pictured as a disordered or melted cubic phase. It is formed by a surfactant bilayer that divides the space into two nonpenetrating solvent regions, which can be either equal in volume (symmetrical phase) or different (asymmetrical phase). The main difference with the cubic phase is the lack of space order and periodicity. In spite of the absence of long range positional order, a characteristic distance  $d$ , which is related to the average size of the passages, can be determined from the position of the intensity peak of the SAXS spectra. It was assumed that  $d$  scales as  $\phi^{-1}$ , the inverse of the bilayer volume fraction of the sample. There are, however, examples of fits to accurate swelling data that do not extrapolate correctly for  $\phi \rightarrow 0$ .

Recently, Engblom and Hyde [12] have proposed a different model where the swelling data are fitted by a polynomial extrapolating to a correct value for small bilayer volume fractions. This paper addresses the issue of swelling of an  $L_3$  phase of a zwitterionic surfactant (tetradecyldimethyl aminoxide) and of its topology estimation. Our results have been interpreted according to the Engblom and Hyde model.

### II. THEORETICAL BACKGROUND

The x-ray spectra of an  $L_3$  phase give a broad peak, at  $q = q_{\max}$ , and exhibit a typical decay as  $I(q) \approx q^{-2}$  indicating the existence of a local bilayer structure [5]. Different models have been proposed to relate  $q_{\max}$  to the characteristic size  $d$  of the  $L_3$  phase scattering.

On the basis of thermodynamic arguments, Teubner and Strey have calculated the following scattering function for microemulsions [6]:

$$I(q) = \frac{a_1}{a_2 + a_3 q^2 + a_4 q^4}, \quad (1)$$

where the parameters  $a_i$  can be written in terms of  $q_{\max}$ , of the scattered intensities at  $q = q_{\max}$  and at  $q = 0$ , and of the mean square fluctuation of the scattering density [6]. From the correlation function leading to this equation, one can find two length scales: one correlation length  $\chi$  and the characteristic size of the random structure  $d$ , which is related to the peak position by  $d = (2\pi/q_{\max})f(a_i)$ , where the factor  $f$  is a function of the  $a_i$ . Spontaneous curvature is not included in this model.

Structural models taking into account the curvature have been considered by different authors [7–9]. For all models, the inverse of the peak position is proportional to the typical size of the random structure.

#### A. Swelling behavior

In the  $L_3$  phases, the analysis of the swelling behavior, i.e., of the dependence of  $q_{\max}$  as a function of the bilayer volume fraction  $\phi$ , has been done with theoretical arguments similar to those used for lamellar phases. It can be understood from a simple plaquette model [5], in which the curvature of the surfactant film occurs along the edges of the plaquettes. The result is qualitatively the same as for lamellar phases:

$$q_{\max} = \alpha \frac{2\pi}{\delta} \phi, \quad (2)$$

where  $\delta$  is the bilayer thickness and  $\alpha$  is a constant. For a lamellar phase  $\alpha=1$ . For a sponge phase, the lattice models lead to  $d=2\pi/q_{\max}$  and  $\alpha\approx 1.5$ , while from experimental results  $\alpha=1.4-1.6$  [5,8,10,11].

A more careful study of the local geometry of the  $L_3$  phase shows that its bilayers are not even locally flat and that the swelling law must be corrected by a cubic term. Engblom and Hyde [12] have calculated a corrected law assuming that the structure of the sponge phase can be locally modeled with an infinite periodic minimal surface (IPMS) [13]. They have also reanalyzed some swelling data from the literature and found a better agreement with their theory. Their results permit us to relate between the swelling data to the topology of the phase, in order to estimate the position of the neutral surface in the surfactant bilayer. This neutral surface is the location at which an imaginary surface describing the film bending energy can be located [14]. It is identified as the surface located at the point where the area per molecule remains invariant during the swelling and plays an important role in explaining the stability of the mesophases. Nevertheless, in the literature one cannot find independent determinations of the swelling behavior and of the topology for the same sponge phase, which precludes the neutral surface location to be exactly estimated.

### B. Topology of the $L_3$ phase

Several models have been suggested in order to establish the topology of an  $L_3$  phase that characterizes the connectivity of its bilayers [15]. All theories assume that the polar-apolar interface forms a surface parallel to an IPMS and require the knowledge of the surfactant chain length, the characteristic size  $d$ , and the composition of the system; some of them require the area per surfactant molecule to be known.

An interesting approach has been provided by Anderson and Wennerström in the framework of self-diffusion of individual particles in the bilayers of cubic and  $L_3$  phases [16]. Assuming that the probe diffuses on an IPMS, a finite element solution of the two-dimensional diffusion equation is computed. The theoretical values of the self-diffusion coefficient  $D_S$  are well fitted by the following expression:

$$\frac{D_s}{D_0} = a - b\phi^2, \quad (3)$$

provided that  $0 < \phi < 0.4$ .  $D_0$  is the diffusion coefficient of the probe in a flat bilayer,  $a = \frac{2}{3}$  (this result is obtained analytically) and  $b$  is a topology-dependent constant, whose values for two minimal surfaces have been computed [16]. They assumed that Eq. (3) remains valid in  $L_3$  phases after melting of the corresponding cubic phase. This is equivalent to assuming that the self-diffusion coefficient  $D_S$  depends only on the local connectivity, i.e., on the number of cells connected to a given unit cell in the structure, which is a reasonable assumption. One also assumes that the connectivity is conserved upon dilution, i.e., that holes in the bilayers are not formed during the dilution. It can be shown that if holes are formed, the  $L_3$  phase will rapidly become unstable [17]. Anderson and Wennerström successfully used Eq. (3) with  $L_3$  phases.

### III. EXPERIMENT

The sponge and lamellar phases are prepared in the ternary system formed by a zwitterionic surfactant (tetradecyldimethyl aminoxide or  $C_{14}$ DMAO), a cosurfactant (hexanol) and water as solvent [18].

The cosurfactant concentration plays a key role in controlling the lamellar-sponge transition: it modifies the spontaneous curvature  $c_0$  of the monolayers forming the bilayer. This spontaneous curvature arises because monolayers are not symmetrical, which is not the case for bilayers where  $c_0^{\text{bil}}=0$ . It can be shown [4] that the spontaneous curvature of the monolayers forming a bilayer is related to the Gaussian elasticity modulus  $\tilde{K}$  of the later by

$$\tilde{K} = (2\tilde{K}_{\text{mono}} - 8tc_0K_{\text{mono}}), \quad (4)$$

where  $\tilde{K}_{\text{mono}}$  and  $K_{\text{mono}}$  are, respectively, the Gaussian and the mean curvature elasticity moduli of the monolayer, and  $t$  is the distance from the midsurface of the bilayers to the neutral surface, which is defined in Sec. II. On the other hand, the bilayer mean curvature elasticity modulus  $K$  is simply  $2K_{\text{mono}}$  and  $c_0$  has no effect on it. In a bilayer system,  $K$  and  $\tilde{K}$  play very different roles [4]: the former regulates the amplitude of thermal bending modes, whereas the latter controls the degree of connectivity of the structure. Strongly negative values of  $\tilde{K}$  favor the formation of disconnected objects, like vesicles, while positive values produce connected structures, like the sponge phase. It is known that increasing the relative cosurfactant concentration in a surfactant system decreases  $c_0$  [19]. So, Eq. (4) shows that, in this case,  $\tilde{K}$  will increase and, as the cosurfactant concentration reaches some critical value, it will favor the formation of the sponge phase [20]. In our  $L_3$  phases, we keep the cosurfactant to surfactant ratio  $r$  constant ( $r=1.05$  in weight); for lower  $r$  values a lamellar phase is observed.

The phase diagram of our ternary system has been extensively studied by Miller *et al.* [18]. The bilayers are slightly charged due to protonation of the aminoxide groups by water [21]. The Debye screening length is of the order of the interlamellar spacing, and electrostatic interactions stabilize the lamellar and sponge phases [21]. The bilayer phases are present in a wide range of surfactant (+ cosurfactant) volume fractions, for a given cosurfactant to surfactant ratio, which controls the lamellar-sponge transition as explained above.

The swelling behavior of the lamellar and  $L_3$  phases has been studied by SAXS. We use a Rigaku rotating anode source that produces the  $\text{Cu } K_\alpha$  lines ( $1.54 \text{ \AA}$ ) with a fine focus ( $1 \text{ mm} \times 0.1 \text{ mm}$ ). The output was collimated by a gold-plated quartz mirror. The linear detector, with 512 channels, was placed 81 cm from the sample position. The resolution of the direct beam was measured to be  $\Delta q = 0.0017 \text{ \AA}^{-1}$  full width at half maximum. In these experiments the collimation corrections are negligible.

In order to get an idea of the  $L_3$  phase topology, the fluorescence recovery after fringe pattern photobleaching (FRAPP) technique is used. A fluorescent probe is homogeneously dissolved in the sample, and an irreversible destruction of the fluorescent groups is carried out by a very short, powerful laser pulse, without modification of the other physical characteristics of the probe. Then, a weak laser beam is

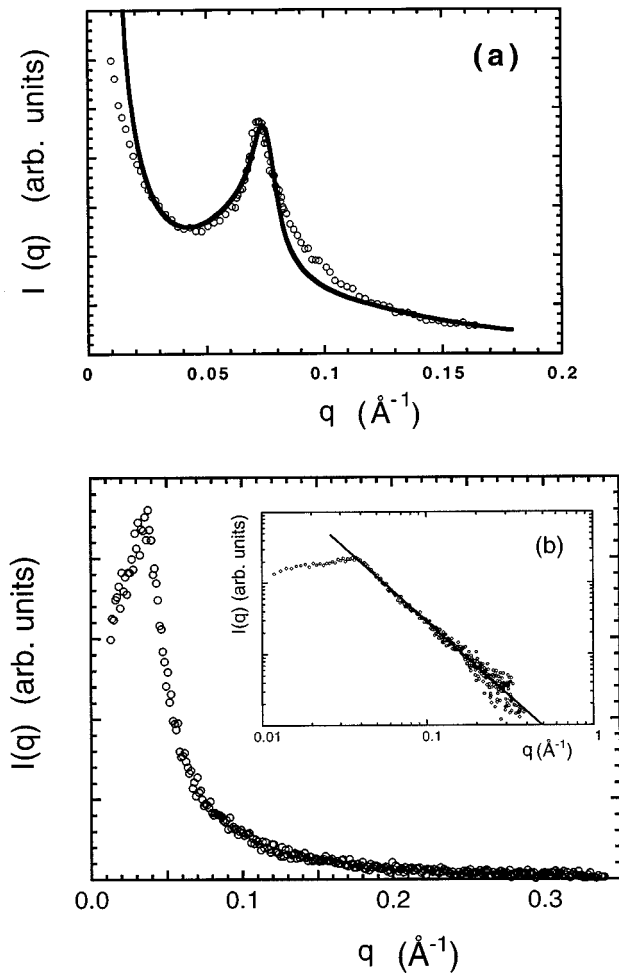


FIG. 1. Typical x-ray spectra for a lamellar (a) and an  $L_3$  (b) phase. For the  $L_\alpha$  phase the continuous line is the best fit to the model of bilayers stabilized by electrostatic interactions [23]. In the inset of (b) a log-log plot for the  $L_3$  phase is shown in order to check the  $q^{-2}$  decaying behavior (the final slope is  $-2.05$ ).

used to monitor the fluorescence signal as diffusion of the probes leads to a new homogeneous concentration in the previously bleached region of the sample. Both the bleaching and the monitoring beams are divided and superposed in the sample to create a fringe geometry. After the bleaching pulse, a piezoelectric crystal causes the monitoring beam to sweep the bleached fringes in the sample, which reduces the noise-to-signal ratio in the recovery exponential signal. The diffusion coefficients are deduced from the characteristic times of the recovery curves with an error smaller than 5%. The samples were put in Hellman quartz cells of 1-mm path length and kept at constant temperature ( $23 \pm 0.1$  °C) during the experiment. More details on the experimental procedures have been published elsewhere [22].

#### IV. RESULTS AND DISCUSSION

##### A. Swelling of the lamellar and sponge phases

A typical x-ray spectrum of an  $L_3$  phase exhibits a broad peak and an  $I(q) \approx q^{-2}$  decay (Fig. 1);  $q_{\max}$  can be easily obtained from visual inspection of the data. For the neighboring lamellar phases ( $r=0.9$ ) a well-defined, sharper peak

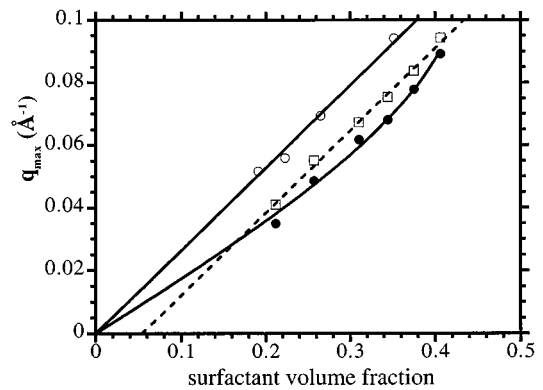


FIG. 2. Swelling behavior of the lamellar (open circles) and  $L_3$  phases (filled circles) of the  $C_{14}$ DMAO-hexanol-water system. In both cases, the experimental error is of the order of the dot dimension. The full lines are theoretical fits: for the lamellar phase to Eq. (2) and for the  $L_3$  phase to Eq. (5). The squares are  $2\pi/d$  versus  $\phi$  values as obtained from the Steubner and Strey model (see text); the linear fits do not extrapolate to the origin.

appears and is well fitted by the model of bilayers stabilized by electrostatic interactions [23], from which we obtain  $q_{\max}$ .

In Fig. 2,  $q_{\max}$  versus  $\phi$  graphs are shown for both the lamellar and the sponge phases. For the lamellar phase, the straight line represents a fit to the classical law [4,10]:  $q_{\max} = (2\pi/\delta)\phi$ , where  $\delta$  is the average bilayer thickness. The agreement between the experimental points and the theoretical fit is good. From the experimental slope, the bilayer thickness  $\delta$  is found to be equal to 23.8 Å. From the  $\delta$  and  $\phi$  values, a simple geometrical model leads to an area per head group of 77.1 Å<sup>2</sup> (one surfactant molecule together with its cosurfactant neighbors).

For the  $L_3$  phase the linear fit is obviously not adequate to describe the swelling behavior. Even if the data could be approximated by a straight line, they would not extrapolate to the origin. This deviation from the classical law [Eq. (2)] could be explained by concentration-dependent corrections due to the finite correlation length, which can be computed in the framework of the Steubner and Strey model developed to explain the scattering when bulk contrast is present. This is obviously not the case in our  $L_3$  phase, since the scattering is due to the contrast between the film and the bulk. Nevertheless, we have fitted all the  $L_3$  spectra with Eq. (1) in order to extract the  $d$  values. The fits to the experimental spectra are rather poor, and the computed swelling laws still do not extrapolate to the origin (Fig. 2).

An alternative approach is to use the theory of Englom and Hyde for a sponge phase of normal curvature, which assumes that a neutral surface, located symmetrically on both sides of the bilayer [12], is maintained during swelling at a certain distance  $t$  from the midsurface. In this case, the swelling follows the cubic equation

$$\phi = c_1 q_{\max} + c_2 q_{\max}^3, \quad (5)$$

where  $c_1$  and  $c_2$  are constants depending on the phase topology. From these constants, the location of the neutral surface can be calculated as follows [12]:

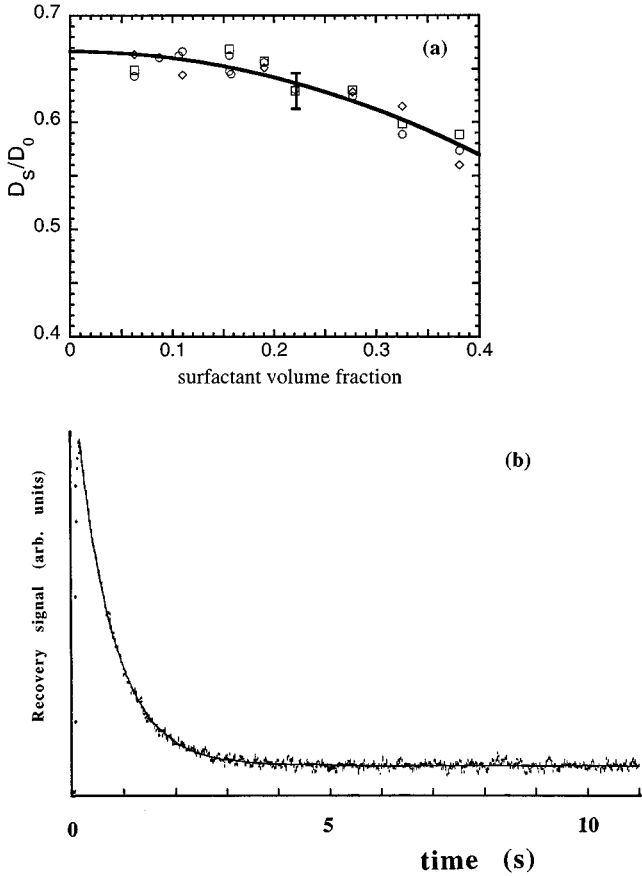


FIG. 3. (a) Normalized diffusion coefficient for the three fluorescein-modified probes in the bilayers of an  $L_3$  phase. The symbols ( $\circ$ ), ( $\square$ ), and ( $\diamond$ ) correspond to a hydrophobic tail with 12, 16, and 18 carbon atoms, respectively. The experimental data gather on a universal curve,  $D_S/D_0 = a - b\phi^2$ , regardless of the structure of the dye. A typical error bar is also shown. (b) represents a single exponential fit to typical FRAPP data.

$$t = \left( -\frac{4\pi^2 H}{\chi} \right)^{1/3} \left( \frac{c_2}{c_1} \right)^{1/2}, \quad (6)$$

where the topological factors  $H$  and  $\chi$  are the so-called homogeneity index and the Euler-Poincaré characteristic per unit cell, respectively [12].  $\chi$  describes the topology of the IPMS; it is related to the genus  $g$  (number of handles) per unit cell by  $\chi = 2(1-g)$ , whereas the homogeneity index  $H$  links the surface area of the IPMS per unit cell  $A_{uc}$  and the volume of the unit cell  $V_{uc}$  to its topology:

$$H \equiv \frac{A_{uc}^{3/2}}{(2\pi\chi)^{1/2} V_{uc}}. \quad (7)$$

In Fig. 2 a fit to Eq. (5) is also plotted for the  $L_3$  phase, showing excellent agreement with the experimental data. At this stage no additional information can be given about the neutral surface because the phase topology is unknown.

### B. Self-diffusion in the sponge phase

In order to provide some information on the topology of the  $L_3$  phase, the self-diffusion coefficient of three fluorescein-modified molecules [24] has been measured by

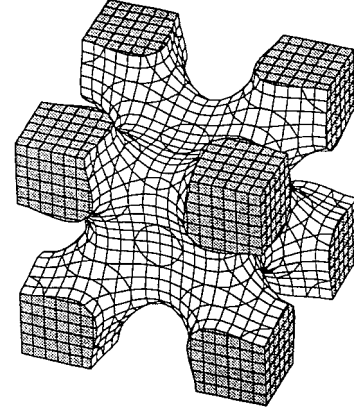


FIG. 4. Conventional unit cell of an approximation to the I-WP periodic minimal surface from Ref. [27]. The parameters obtained from the fits with Eq. (1) indicate that this is the closest topology to our  $L_3$  samples.

the FRAPP technique, as a function of the bilayer volume fraction. All these molecules have the same fluorescent polar head, but a different hydrophobic tail. They all have the same  $D_S/D_0$  for a given surfactant volume fraction (Fig. 3); this ensures that the probe remains within the bilayers [25]. In Fig. 3 the  $D_S/D_0$  versus  $\phi$  values are depicted on a universal curve for the three fluorescein-modified molecules diffusing in the bilayers of an  $L_3$  phase. In the dilute regime, the diffusion coefficient is nearly constant in agreement with previous results [26]; however, in the more concentrated regime the diffusion coefficient decreases as  $\phi$  increases.

The experimental points ( $D_S$  versus  $\phi$ ) are fitted to Eq. (3) and a remarkable agreement between experiment and theory is observed. The predicted  $D_0$  coefficients are easily calculated from the fits if we suppose a cubic symmetry, i.e.,  $a = \frac{2}{3}$ . This value of  $a$  has been verified by measuring  $D_0$  for one probe in the neighboring lamellar phase. We have  $a = 0.68 \pm 0.05$  in agreement with theory and previous results [26].

In principle, from the experimental  $b$  value, one can infer the minimal surface topology that better describes our  $L_3$  phase. To our knowledge, the  $b$  value has been calculated only for two topological families of cubic phases formed by bilayers. These values are  $b = 0.45$  and  $b = 0.6$  for the P and the I-WP families, respectively [16]. P stands for the Schwarz primitive surface, and I-WP for the wrapped-package one (I denotes a body-centered structure, see Fig. 4) [27].

Even if the  $b$  values of more topological families are needed in order to unambiguously assign a topology to our phases, it is interesting to explore the implications of our experimental results. From the data, it can be seen that the  $b$  value ( $0.607 \pm 0.048$ ) seems nearer to that of the I-WP family. A unit cell of an approximation to this periodic minimal surface is shown in Fig. 4; its Euler-Poincaré characteristic per unit cell  $\chi$  is  $-6$  (i.e., its genus is 4) and its homogeneity index  $H$  is 0.7425. With these results in mind, one can assume that the studied  $L_3$  phase is described by the I-WP minimal surface and thus calculate the displacement of the neutral surface from the midsurface of the bilayer using Eq. (6). The resulting value is  $t \approx 9 \text{ \AA}$ , which indicates that, in

this case, the neutral surface would lie near the polar-apolar interface of the bilayer.

### V. CONCLUSION

The swelling behavior of the  $L_3$  phase of the  $C_{14}$ DMAO-hexanol-water system is well described by the law found for the swelling of minimal surfaces [12]. In principle, self-diffusion experiments can provide an independent estimation of the topology of the system. If we compare the available theoretical results to our experimental data, the  $L_3$  phase topology seems to be close to that of the I-WP minimal surface. With this assumption, we were able to locate the

position of the neutral surface near the polar-apolar interface of the bilayer. Additional theoretical values of  $b$  [defined in Eq. (3)] are necessary to assign unambiguously the exact topology of the  $L_3$  phase from the  $D_s$  versus  $\phi$  data.

### ACKNOWLEDGMENTS

It is a pleasure to thank H. Hoffmann and M. Gradzielski for the gift of  $C_{14}$ DMAO and M. Waks and E. Perez for a careful reading of the manuscript. A.M. acknowledges financial support from the Consejo Nacional de Ciencia y Tecnología (Conacyt), Mexico.

- 
- [1] *Physics of Amphiphilic Layers*, edited by J. Meunier, D. Langevin, and N. Boccaro (Springer-Verlag, Berlin, 1987).
- [2] K. Fontell, *Colloid Polym. Sci.* **268**, 224 (1990); K. Larsson, *J. Phys. Chem.* **93**, 7304 (1989); V. Luzzati, R. Vargas, P. Mariani, A. Gulik, and H. Delacroix, *J. Mol. Biol.* **229**, 540 (1993).
- [3] P. Barois, S. T. Hyde, B. W. Ninham, and T. Dowling, *Langmuir* **6**, 1136 (1990).
- [4] G. Porte, *J. Phys. Condens. Matter* **4**, 8649 (1992).
- [5] G. Porte, J. Marignan, P. Bassereau, and R. May, *J. Phys. (France)* **49**, 511 (1988).
- [6] M. Teubner and R. Strey, *J. Chem. Phys.* **87**, 3195 (1987).
- [7] M. E. Cates, D. Roux, D. Andelman, S. T. Milner, and S. A. Safran, *Europhys. Lett.* **5**, 733 (1988).
- [8] D. Roux, C. Coulon, and M. E. Cates, *J. Phys. Chem.* **96**, 4174 (1992).
- [9] T. Zemb, in *Neutron, X-ray and Light Scattering*, edited by P. Lindner and T. Zemb (North-Holland, Amsterdam, 1991).
- [10] M. Skouri, J. Marignan, J. Appell, and G. Porte, *J. Phys. II (France)* **1**, 1121 (1991).
- [11] D. Gazeau, A. M. Bellocq, D. Roux, and T. Zemb, *Europhys. Lett.* **9**, 447 (1989).
- [12] J. Engblom and S. T. Hyde, *J. Phys. II (France)* **5**, 171 (1995).
- [13] J. C. C. Nitsche, *Lectures on Minimal Surfaces* (Cambridge University, Cambridge, 1989), Vol. 1.
- [14] H. Chung and M. Caffrey, *Biol. J.* **66**, 377 (1994).
- [15] S. T. Hyde, *J. Phys. Chem.* **93**, 1458 (1989); D. C. Turner, Z.-G. Wang, S. M. Gruner, D. A. Mannock, and R. N. McElhaney, *J. Phys. II (France)* **2**, 2039 (1992).
- [16] D. M. Anderson and H. Wennerström, *J. Phys. Chem.* **94**, 8683 (1990).
- [17] C. K. Bagdassarian, D. Roux, A. Ben-Shaul, and W. M. Gelbart, *J. Phys. Chem.* **94**, 3030 (1991).
- [18] C. A. Miller, M. Gradzielski, H. Hoffmann, U. Krämer, and C. Thunig, *Progr. Colloid. Polym. Sci.* **84**, 1 (1991).
- [19] Y. Hendrickx, J. Charvolin, and M. Raviso, *J. Colloid Interface Sci.* **100**, 597 (1984).
- [20] G. Porte, J. Appell, P. Bassereau, and J. Marignan, *J. Phys. (France)* **50**, 1335 (1989).
- [21] C. Thunig, H. Hoffmann, and G. Platz, *Prog. Colloid Polym. Sci.* **79**, 297 (1989).
- [22] D. Chatenay, W. Urbach, C. Nicot, M. Vacher, and M. Waks, *J. Phys. Chem.* **91**, 2198 (1987).
- [23] F. Nallet, R. Laversanne, and D. Roux, *J. Phys. II (France)* **3**, 487 (1993).
- [24] More details are planned for future publication.
- [25] B. Lindman, U. Olsson, and H. Wennerström, *Langmuir* **9**, 625 (1993).
- [26] A. Ott, W. Urbach, D. Langevin, and H. Hoffmann, *Langmuir* **8**, 345 (1992).
- [27] S. T. Hyde, *J. Phys. Colloq. (Paris)* **51**, C7-209 (1990).